Signal Level Distributions and Fade Event Analyses for a 5 GHz Microwave Link Across the English Channel

D.R. Wortendyke

A.P. Barsis

R.R. Larsen

TABLE OF CONTENTS

LIST OF FIGURES

LIST OF TABLES

v

SIGNAL LEVEL DISTRIBUTIONS AND FADE EVENT
ANALYSES FOR A 5 GHz MICROWAVE LINK
ACROSS THE ENGLISH CHANNEL

D.R. Wortendyke*, A.P. Barsis*, and R.R. Larsen**

This report describes instrumentation for fading
studies and measurement results over an 88-km
multiple-diversity line-of-sight microwave link
across the English Channel operating in the
4 to 5 GHz frequency range. Signal level and
fade duration statistics derived from the measure-
ments are compared with CCIR models. It is found
that median fade duration tends to be less than
estimates from the CCIR models.

Key words: Microwave fading, multiple diversity
            receivers, 5 GHz signal levels, auto-
            matic signal monitoring.

1.   INTRODUCTION

The Institute for Telecommunication Sciences (ITS) of the
National Telecommunications and Information Administration
U.S. Department of Commerce was tasked in 1972 by the U.S. Air
Force Communications Service (AFCS) to develop automated test and
acceptance procedures and equipment to simplify and accelerate
the collection of test and performance data from Defense Communi-
cation Systems (DCS) microwave links. Emphasis was first on
measurement and analyses of received signal level data. Initially,
ITS developed a calculator-based instrument (RSL-1) in 1973,
which was used on the "SCOPE" communication links in Germany and
as a measurement-analysis tool at AFCS Headquarters. Later, a
more sophisticated instrument for received signal level (RSL)
measurements and analysis was developed by ITS. The present
report deals with the utilization of this instrument in a long-
term study and evaluation of propagation effects on a multi-
diversity microwave link across the English Channel between

*The authors are with the National Telecommunications and Infor-
mation Administration, Institute for Telecommunication Sciences,
U.S. Dept. of Commerce, Boulder, CO 80303.

**The author is with the 1842nd Electronics Engineering Group,
United States Air Force, Scott Air Force Base, IL 62225.

terminals near Dover, England, and Houtem, Belgium. This link is
88 km long (with 65 km over water), and operates in the 4 to 5
GHz frequency range. It is a portion of the DCS European network,
and has been carrying traffic since mid-1974.

This report presents first a description of the path, its
implementation, and a brief outline of the RSL-2 instrumentation.
Next is a discussion and analysis of measurement results from a
1-year operating period. Statistics of signal level and fade
events are presented, and the results will also be evaluated for
applicability to similar links.

2. MICROWAVE SYSTEM DESCRIPTION AND IMPLEMENTATION

As shown in Figure 1, the western terminal of the 88-km
link is at Swingate, near Dover, England, on top of the White
Cliffs. The eastern terminal is approximately 19 km inland from
the Channel coast near Houtem, Belgium. The path profile with
antenna positions, heights above mean sea level (in meters), and
a representation of the sea surface for two values of the
effective earth radius factor, k, is shown in Figure 2. Anten-
nas A and B at each terminal are 4.6 m parabolic reflectors, and
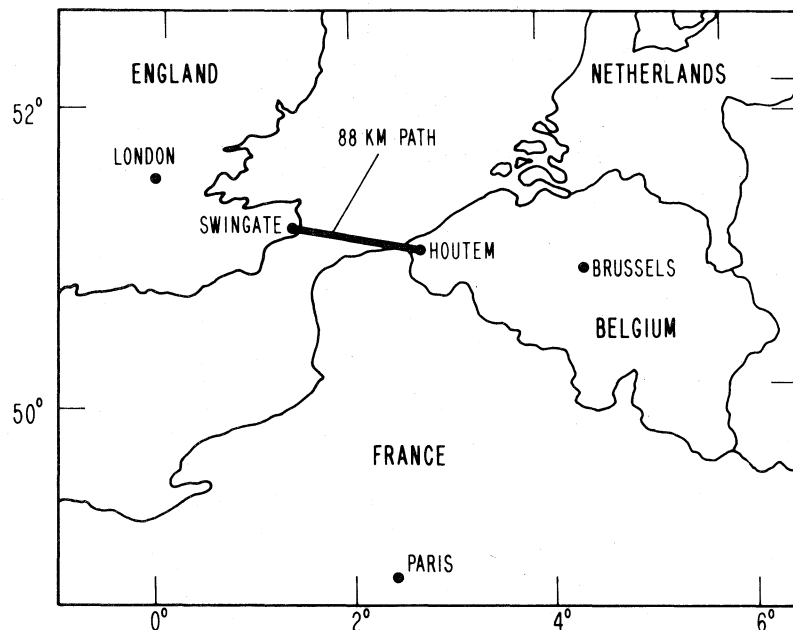antennas C and D are 3.7 m parabolic reflectors.

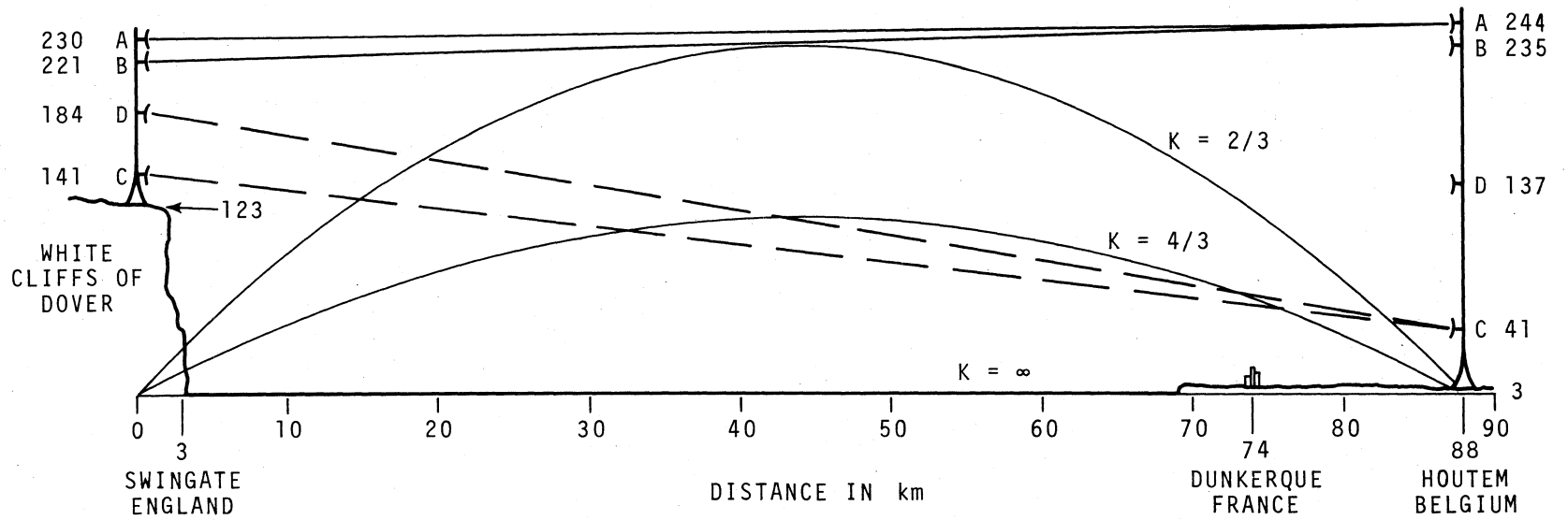Figure 1. Location map for 5 GHz microwave link.

2

Figure 2. Terrain profile for 5 GHz microwave link.

The design considerations for the multiple diversity system were described in detail by Zebrovitz (1975). For sub-refractive and normal conditions ($2/3 \leq k \leq 4/3$), dual diversity operation is provided by paths A and B. For the top path A, clearance amounts to approximately the 11th or 12th Fresnel zone for $k = 4/3$, but it is only a small fraction of the first Fresnel zone (less than 0.1) for $k = 2/3$. Under these conditions, the lower paths (C and D) contribute relatively little to the quadruple diversity combiner input since direct line of sight for these lower paths is blocked by the sea surface. However, when signals from the upper antennas are subject to severe multipath fading because of superrefractive conditions ($k > 4/3$), the lower paths C or D may be within the superrefractive layer with very little attenuation. They would then be expected to provide the principal contribution to the combiner. The lower path C, as an example, becomes grazing for $k = 1.82$.

Two of four transmitters are used as standbys at any specific time, and up to four usable signals at a time are provided to the combiner. It was anticipated that this design would fulfill the performance requirements in terms of signal level and noise power ratio for at least 99.99% of the time.

3. DATA COLLECTION EQUIPMENT

The RSL-2 measurement instrument is a minicomputer-controlled device designed to handle great quantities of time-variant data. The conceptual operation is shown in Figure 3; it is controlled by software programs core-resident in the 24-k word memory. Four dc voltages, proportional to the received signal levels from each of four receivers, are measured every 0.1 s by a 12-bit A-D converter. The mini-computer sorts each of the four measurement values against a stored calibration curve for the particular receiver and then places the data in a histogram with 20 partitions that are equally spaced across the receiver dynamic range. Once per hour the histograms are stored with a date-time-group and the process begins again. A five-point cumulative distribution (signal levels in dBm exceeded for 10%, 50%, 90%, 99%,

4

SWINGATE

FROM HOUTEM

LC-4 RADIO	LC-4 RADIO
REC A	REC C
REC B	REC D

QUICK LOOK STATISTICS
ONCE/HOUR
ON 1-1/2" TTY PAPER
FOR 4 RECEIVERS
AND COMBINED SIGNAL

TTY

RSL-2

PROCESS, SORT,
AND STORE DATA

MINICOMPUTER,
C.I.U., AND
VOLTMETERS

4
REAL-TIME GRAPHS
OF RSL
DURING FADES

6" PAPER/MIN

PRINTER/PLOTTER

36,000 DATA POINTS EACH HOUR RECORDED FOR
EACH CHANNEL

ONE MONTH'S DATA/CASSETTE   FADE DATA

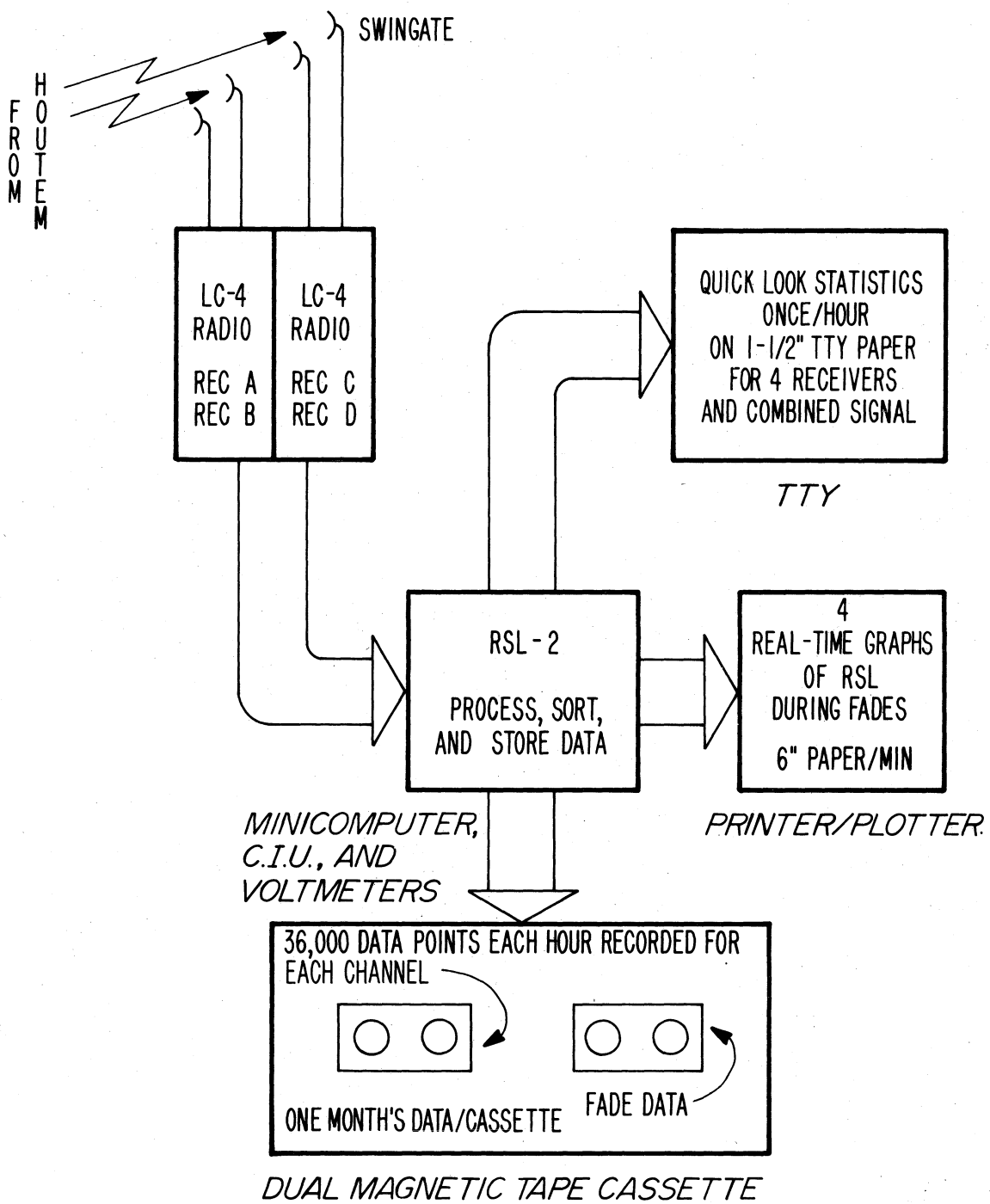*DUAL MAGNETIC TAPE CASSETTE*

Figure 3. Data flow diagram for RSL-2 recording
           system.

5

and 99.9% of the hour) for each of the histograms is also printed out each hour. This is called a quick-look analysis and an example is shown in Table 1. Also, a simulated distribution for all four channels is computed by additive combination of signal power and listed in the right hand column of the printout; it represents optimum system performance, provided all radio hardware (particularly the combiner circuitry) is properly functioning and adjusted. If the signal level fades below a pre-set threshold for the normally line-of-sight upper two paths on receiver A or B, a fully annotated, calibrated, digital, 4-channel strip chart is printed on a printer-plotter for the duration of the fade plus a pre-set 1-min interval.* Chart speed is 6 in/min. An example is shown in Figure 4 that also illustrates the relatively high and steady signals over the lower paths C and D occurring frequently when the signal over paths A and B is in deep fades.

Table 1. Sample Printout for Hourly "Quick-look"
Analysis - Distribution Levels in dBm

% Time That Level is Exceeded	Recvr A	Recvr B	Recvr C	Recvr D	Combined
10%	-43	-40	-34	-37	-31
50%	-46	-43	-37	-40	-34
90%	-55	-58	-40	-43	-37
99%	-70	-70	-52	-46	-37
99.9%	-79	-82	-55	-49	-40

The measured data are stored in a buffer for 10 s, and the output to the printer-plotter is taken from the oldest of the buffered data. Thus, the displays start prior to the leading edge of the fade. At the end of the fade interval (fade duration plus 1 min) the histograms, with starting and ending times, are recorded in a file on a magnetic tape cassette. Hourly data histograms and calibrations are recorded periodically on tape for later evaluation. Each of these cassette tapes can store one month of data. The fade tape capacity is 340 "events" regardless of duration.

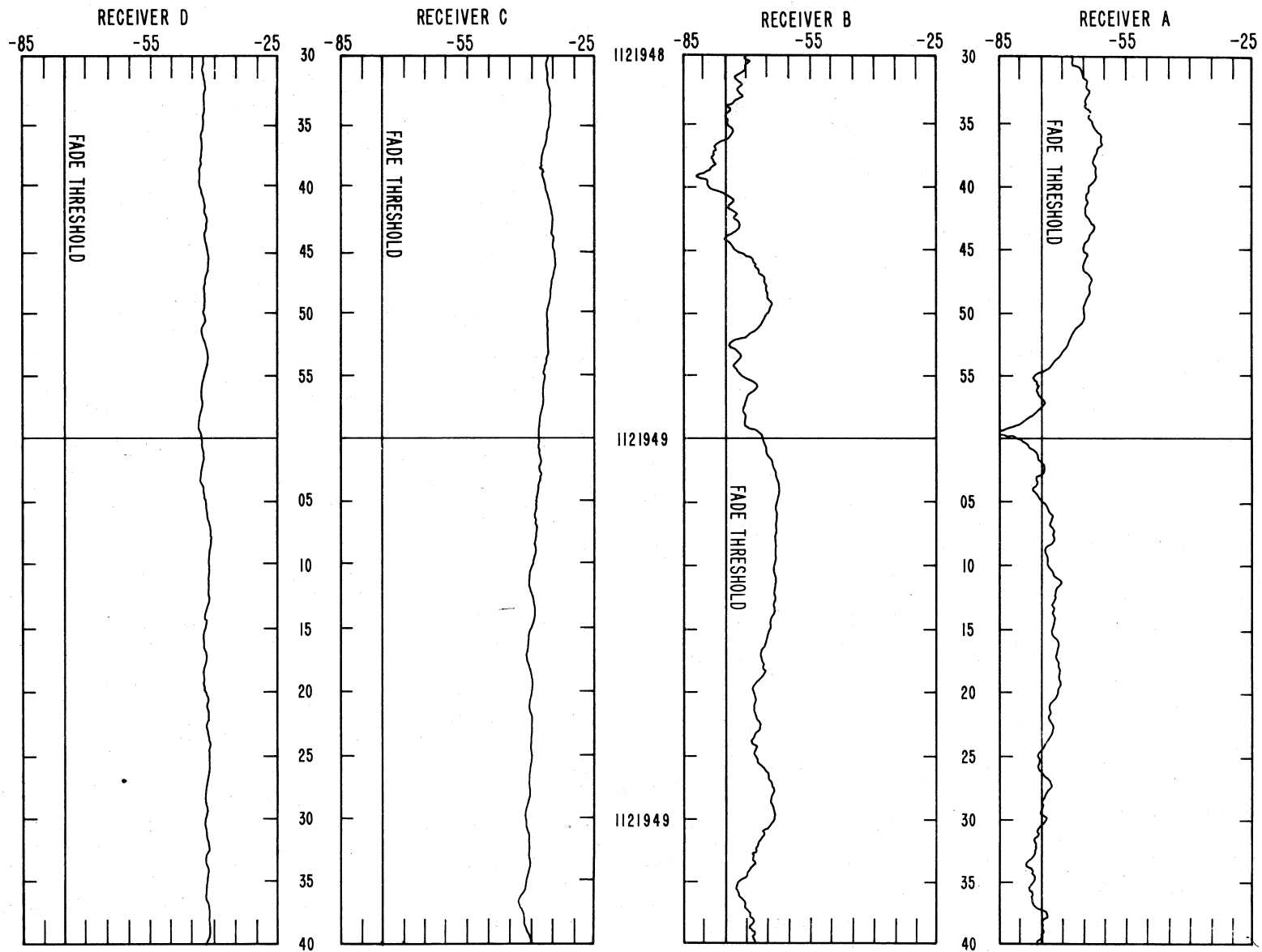*The effect of this delay on fade duration statistics will be discussed in Section 4.3.

Figure 4. Sample of digital strip chart recording.

Data acquisition and sorting is done in about 10 ms, leaving 90 ms between clock ticks available for other tasks such as further processing when the teleprinter is not actually printing any data. Processed data include a histogram and cumulative distributions of received signal levels for any hour, day, month, or fade period. Any set of calibration voltages may be read from the monthly tape for quality assurance checks of system performance.

4. MEASUREMENT RESULTS

Signal level distributions and fade event statistics were obtained over the period from mid-July 1974 to the beginning of June 1975. During this time, the radio system and the RSL-2 equipment were operating for approximately 3650 hrs distributed over the entire year so that all seasons are represented. This constitutes the data base for the analyses of signal level distributions and fade duration.

4.1 Signal Level Distributions

Figure 5 is a plot of instantaneous signal level distributions for all four receivers obtained from the RSL-2 equipment at the rate of 10 data points per second. Approximately 130×10^6 samples for each receiver are represented here. The data are plotted on Rayleigh paper and compared with the theoretical Rayleigh distribution. Qualitatively, the approximation appears to be good for the data from the line-of-sight paths (receivers A and B) suggesting multi-component multipath as the principal cause of fading. The data from receivers C and D deviate substantially from the Rayleigh distribution, and the effect of super refraction during small percentages of time is quite evident from the steep rise of the curves toward the free-space level of -32.9 dBm for small percentages of time. The graph also shows the calculated distribution for all signal powers combined additively (see the discussion in Section 3 in conjunction with Table 1). The apparent system performance improvement is about 12 dB for 99.9% of the time over the performance of a single
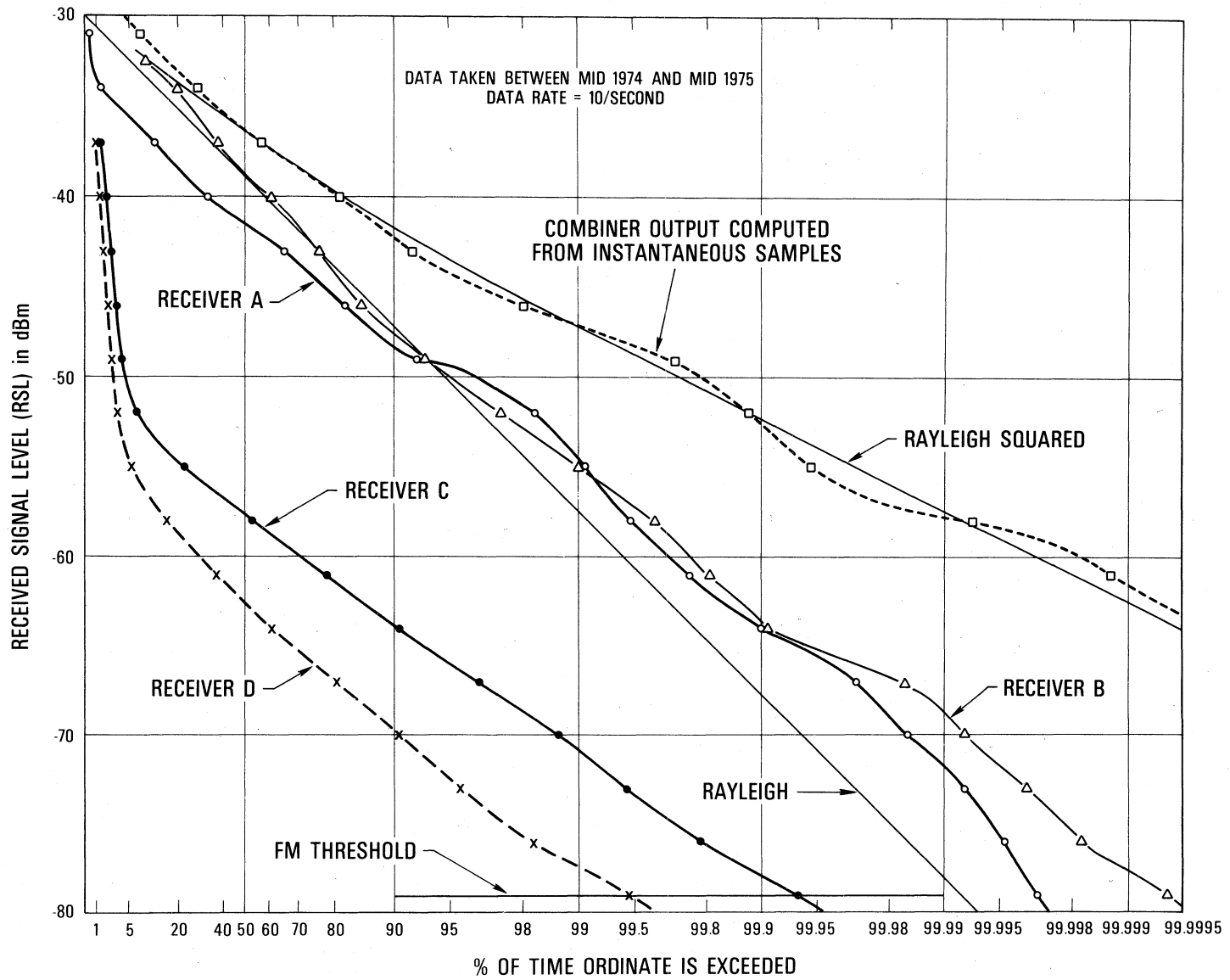
Figure 5. Received signal level distributions (all data).

line-of-sight path. This combined distribution follows the
"Rayleigh squared" curve as postulated by White for uncorrelated
fading (White, 1970).

From the system parameters (Zebrovitz, 1975), the received
signal level corresponding to line-of-sight transmission through
the atmosphere without the effects of reflections or multipath
is -32.9 dBm. The parameters are listed in Table 2 below.
Figure 5 shows that the median received signal levels over the
measurement period differ from this value: they are -38.7 dBm
for receiver A, and -41.3 dBm for receiver B. This discrepancy
as well as the difference between the results from the two
receivers may be caused by uncertainties in equipment param-
eters, antenna alignment, and possibly by path or atmospheric
parameters not considered in the calculations.

Table 2. Path and Equipment Parameters

Pathlength:	87.84 km
Carrier frequency (mean for receivers A and B):	4.908 GHz
Free-space basic transmission loss:	145.1 dB
Antennas:	4.57 m (15 ft) paraboloids
Antenna gain:	44.8 dB (relative to isotropic)
Transmitter power:	6.3 W (+38 dBm)
Estimated wave guide and related losses:	14.5 dB
Average atmospheric absorption:	0.8 dB
Estimated average annual mean temperature:	10° C

4.2 Comparisons With Fading Models.

Prediction models for fade depth distributions over micro-wave line-of-sight links have been developed by a number of workers (Barnett, 1972; Morita, 1970). At the XIV Plenary Assembly of the CCIR, useful formulations of these models were adopted and included in Report 338-3 (CCIR, 1978). This formulation is based on a general expression with specific constants for Japan, Northwest Europe, and the United States, and is intended to be valid for the "worst fading month". Consequently, the probabilities of fade occurrence calculated in this manner should be converted from "worst month" to "all year" for comparison with the data described here. Vigants (1975) suggests a procedure for doing this calculation as a function of the annual mean temperature over the path.

Using the applicable path parameters from Table 2, the model distributions were calculated in accordance with the CCIR formulation for Northwest Europe and plotted together with data points for receivers A and B as shown in Figure 6, but only those for deep fades (at least 20 dB below the yearly measured median) where the Rayleigh distribution postulated by the models (CCIR, 1978) is most applicable. Agreement between the data and the model distributions is reasonable but illustrates the uncertainty in extrapolating from "worst month" to "all year" on the basis of an annual mean temperature only. In fact, the data tabulations do not suggest a particular "worst month"; fading is distributed rather uniformly over the year.

Zero reference for the ordinate in Figure 6 is the mean of the yearly median signal levels derived from the receiver A and receiver B measurements (see Figure 5).

Additional calculations have shown that the model given in CCIR Report 338-3 (1978) is not applicable to this path since it greatly overestimates fading occurrence. This is not surprising since this model was derived primarily from data for much shorter overland paths in the midwestern United States.
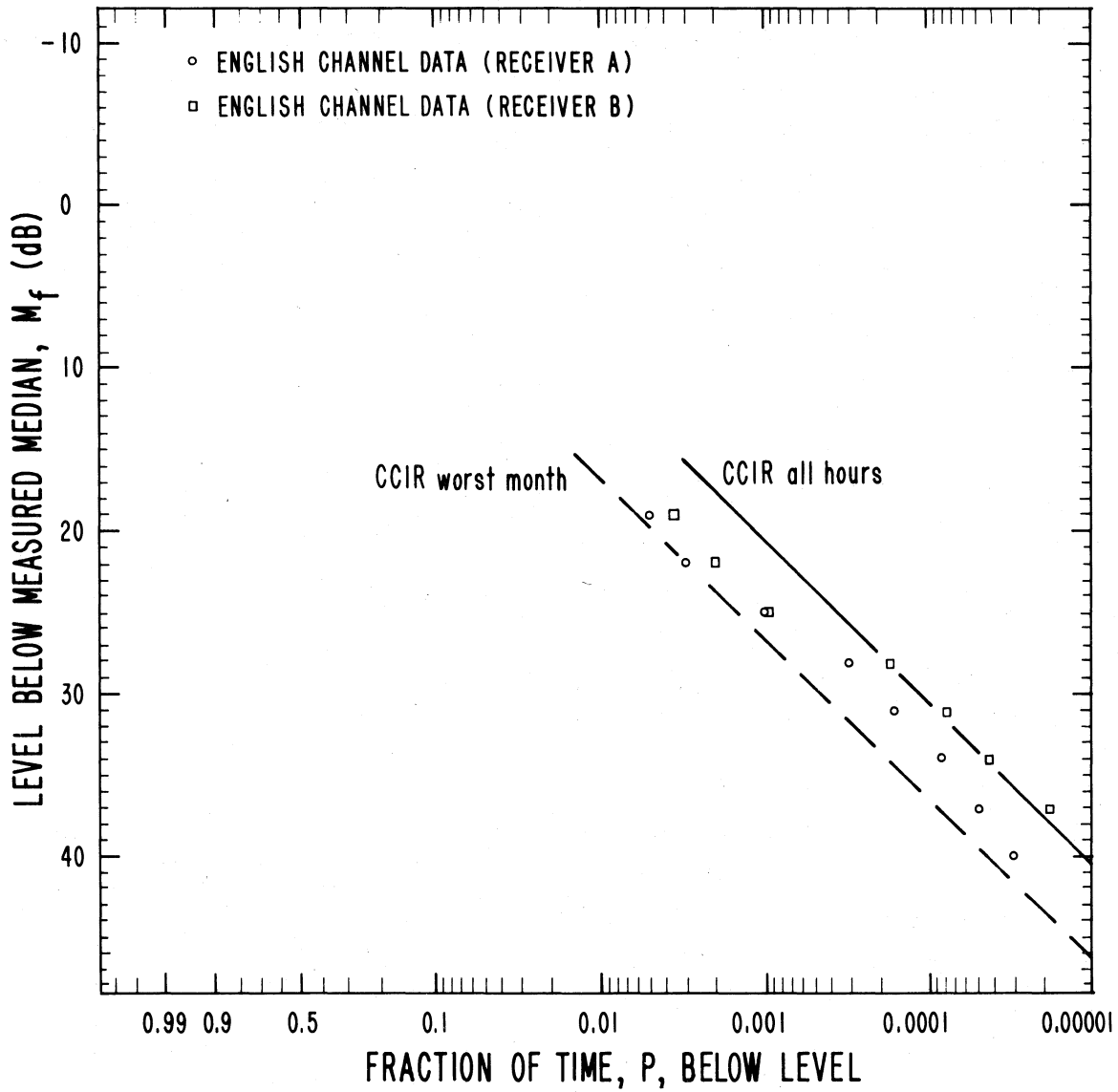
11

Figure 6. Comparison of measurement results with CCIR signal level predictions.

12

4.3 Fade Event Durations.

As explained in Section 3, the RSL-2 equipment automat-
ically acquires, stores, and calculates statistics of fade
event duration at pre-set received signal levels. Data were
obtained throughout the measurement period for receivers A
and B; i.e., for the line-of-sight paths between the high
antennas (see Figure 2). The pre-set fade threshold for all
data was -75 dBm which is 35 dB below the average of the
all-year signal level medians for the two receivers.

The recording and analysis routine inherent in the RSL-2
equipment emphasizes what we choose to call "fade events"
rather than individual fades. The start of a fade event is
defined as that instant when the received signal level from
either receiver A or receiver B drops below the -75 dBm
threshold. The computer then sorts and stores signal level
histograms for all four receivers until one minute after sig-
nals from receivers A and B have both risen above the thres-
hold levels and have remained there. It records the total
elapsed time for receivers A and B signals at and below the
threshold level, and the total length of the fade <u>event</u> cor-
recting for the one-minute time lag. A fade event may include
individual fades on both channels.

The time lag was introduced to allow for limitations in
the peripheral hardware (particularly the tape drive); the
recording mechanism cannot completely follow a number of short
fades in rapid succession. This limitation introduces a
significant bias (against short fades) in the statistical
evaluation of the present data.

Thus, any additional deep fade below the threshold level
that occurs within the one-minute period after the first rise
above the threshold is not evaluated separately, but recorded
as part of the original fade. Consequently, any number of
short fades separated by less than one minute are lumped into
one single longer fade event. Processing methods inherent in
the computer and used for the original data recording methods

13

make it impossible to recover the number and durations of the individual fades when separated by less than one minute. Inspection of available graphic printouts suggest that many of the fades were indeed isolated; i.e., separated by at least one minute. However, Figure 7 shows an example of multiple fades of short duration (about 1 s or less) within a single fade event lasting approximately 45 seconds.

Figures 8, 9, and 10 show cumulative distributions of fade _event_ durations obtained in the manner described above. These distributions are plotted on a log-normal grid; i.e. the absissas are linear in terms of 10 times the logarithm (to the base 10) of the fade event durations in seconds. Because of the bias introduced by the recording method, the total number of individual fades is greater than the number of fade events and and their duration may be appreciably shorter as will be shown later. The distributions are categorized into "time blocks" for winter (Figure 8) and summer (Figure 9) which were introduced originally by Norton, et al. (1955) to evaluate tropospheric propagation data.* These categories provide an indication of diurnal and seasonal changes in the fade event duration distributions. Summary statistics for fade event durations are given in Table 3 below. Similarly, overall cumulative distributions for all hours - winter, all hours - summer, and all hours of the year are shown in Figure 10 with the statistics also listed in Table 3. It is quite evident that the median fade event _durations_ are substantially greater in winter than in summer. However, there are almost twice the _number_ of fade events in summer than in winter (781 versus 414). Nevertheless, the total time in fades of 35 or more dB below the yearly median signal level is still greater in winter than in summer.

---

*The winter time block comprises November through April, and the summer time block May through October.
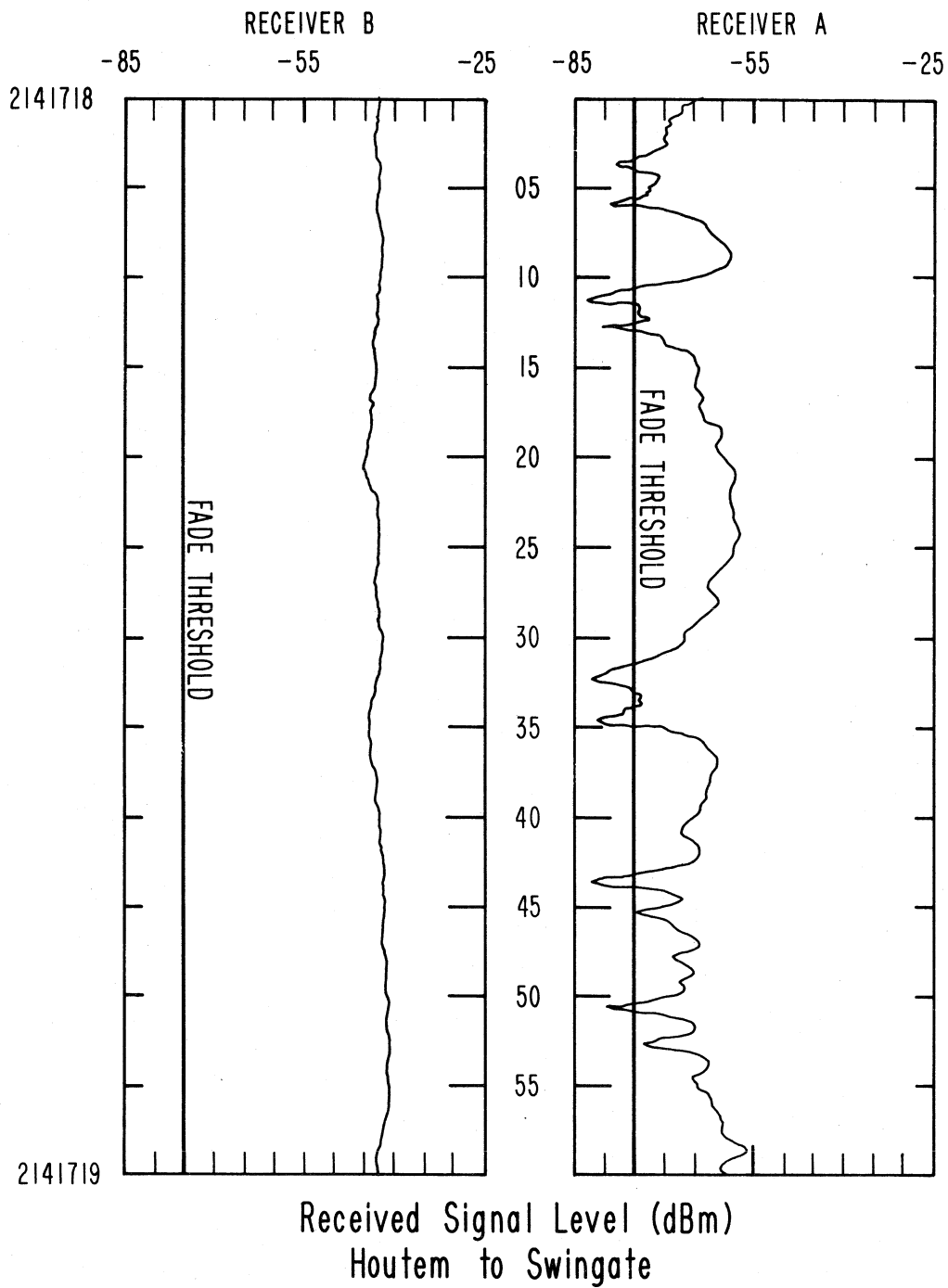
Figure 7. Example of multiple fades within a single
fade event.
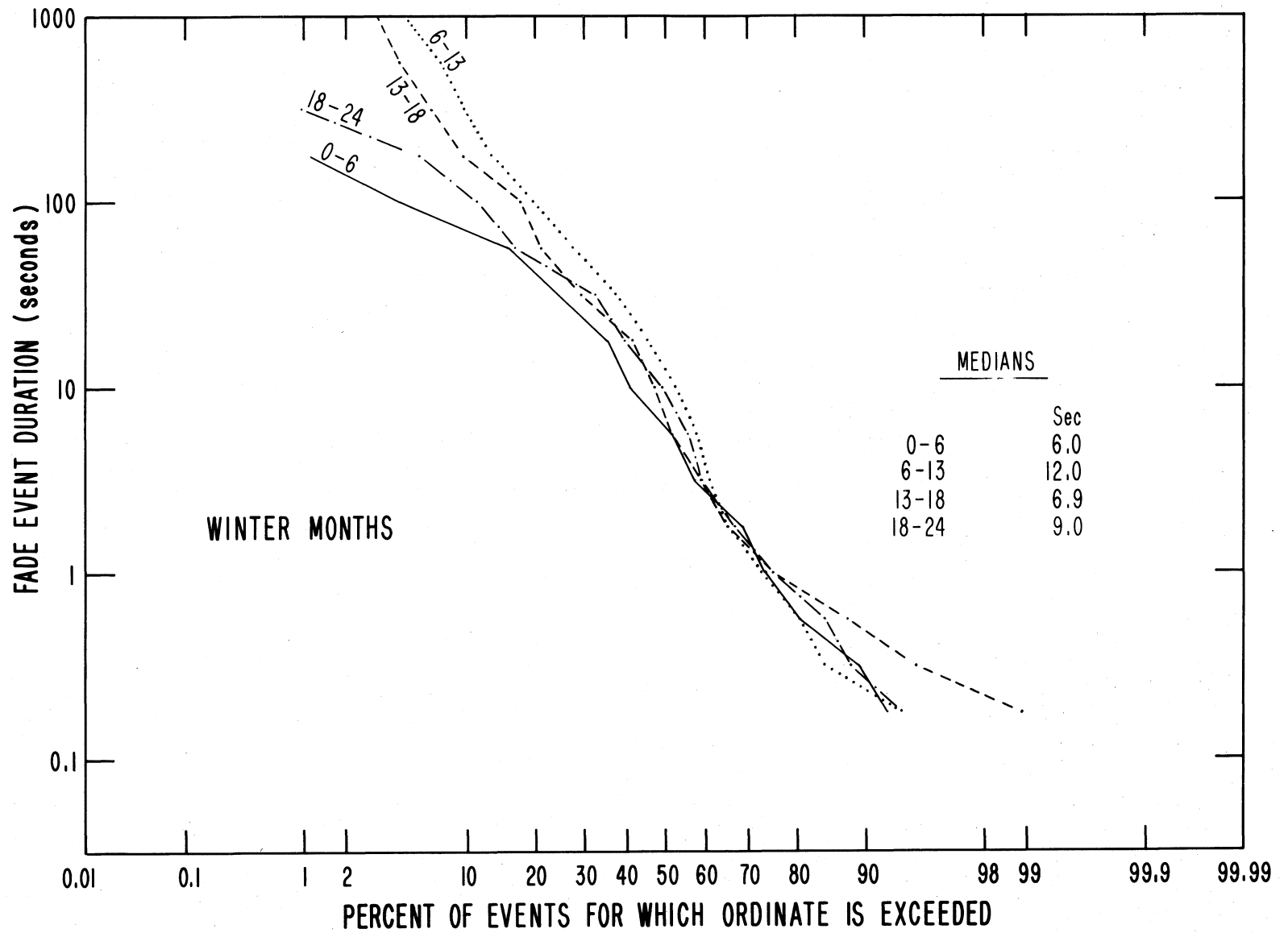
Figure 8. Fade event duration distributions for winter time blocks.

FADE EVENT DURATION (seconds)

1000

100

13-18
18-24
0-6
6-13

MEDIANS

	Sec
0-6	3.16
6-13	1.46
13-18	2.0
18-24	2.57

10

1

SUMMER MONTHS

0.1

0.01   0.1   1   2   10   20 30 40 50 60 70 80   90   98 99   99.9   99.99

PERCENT OF EVENTS FOR WHICH ORDINATE IS EXCEEDED
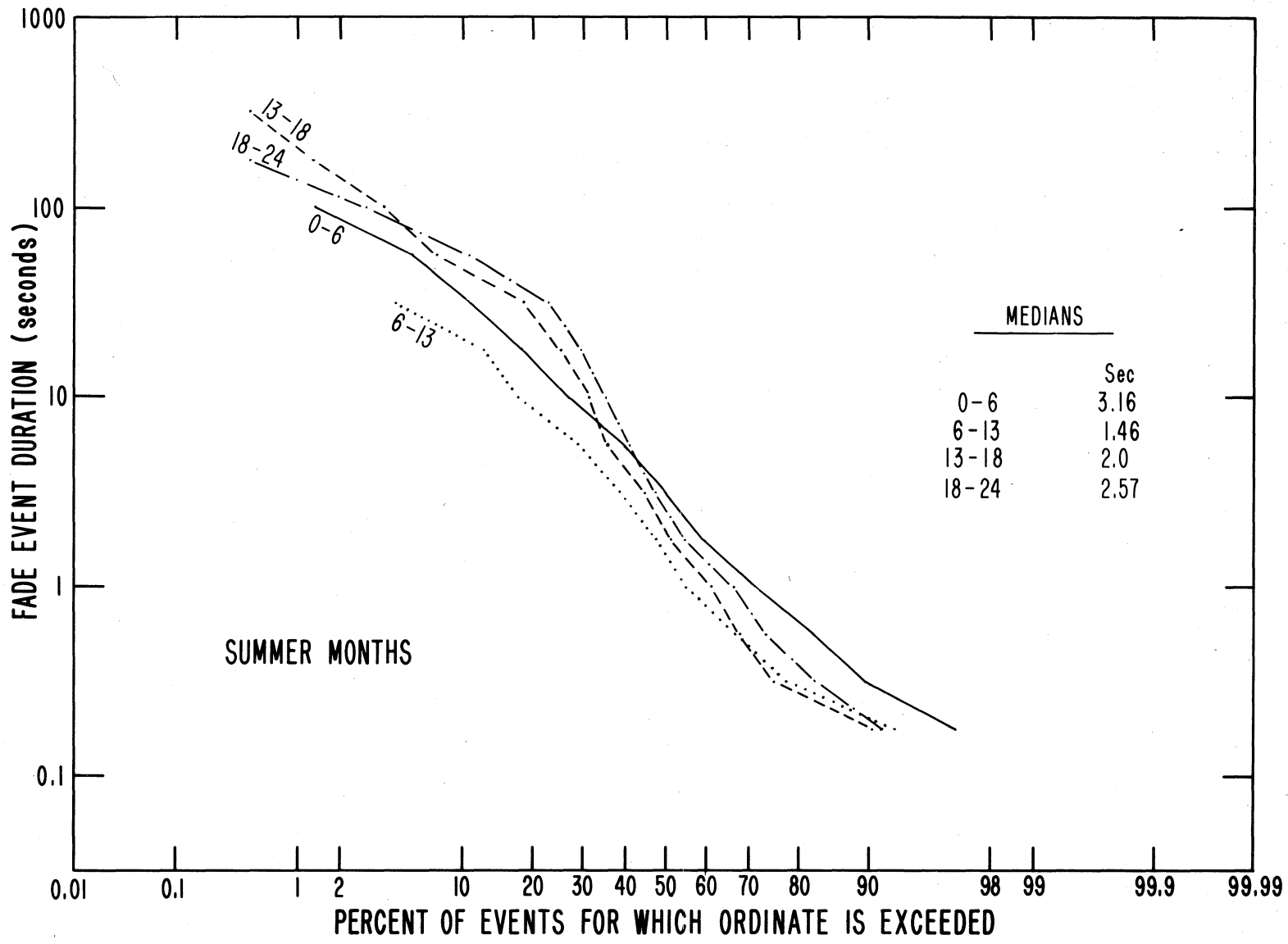
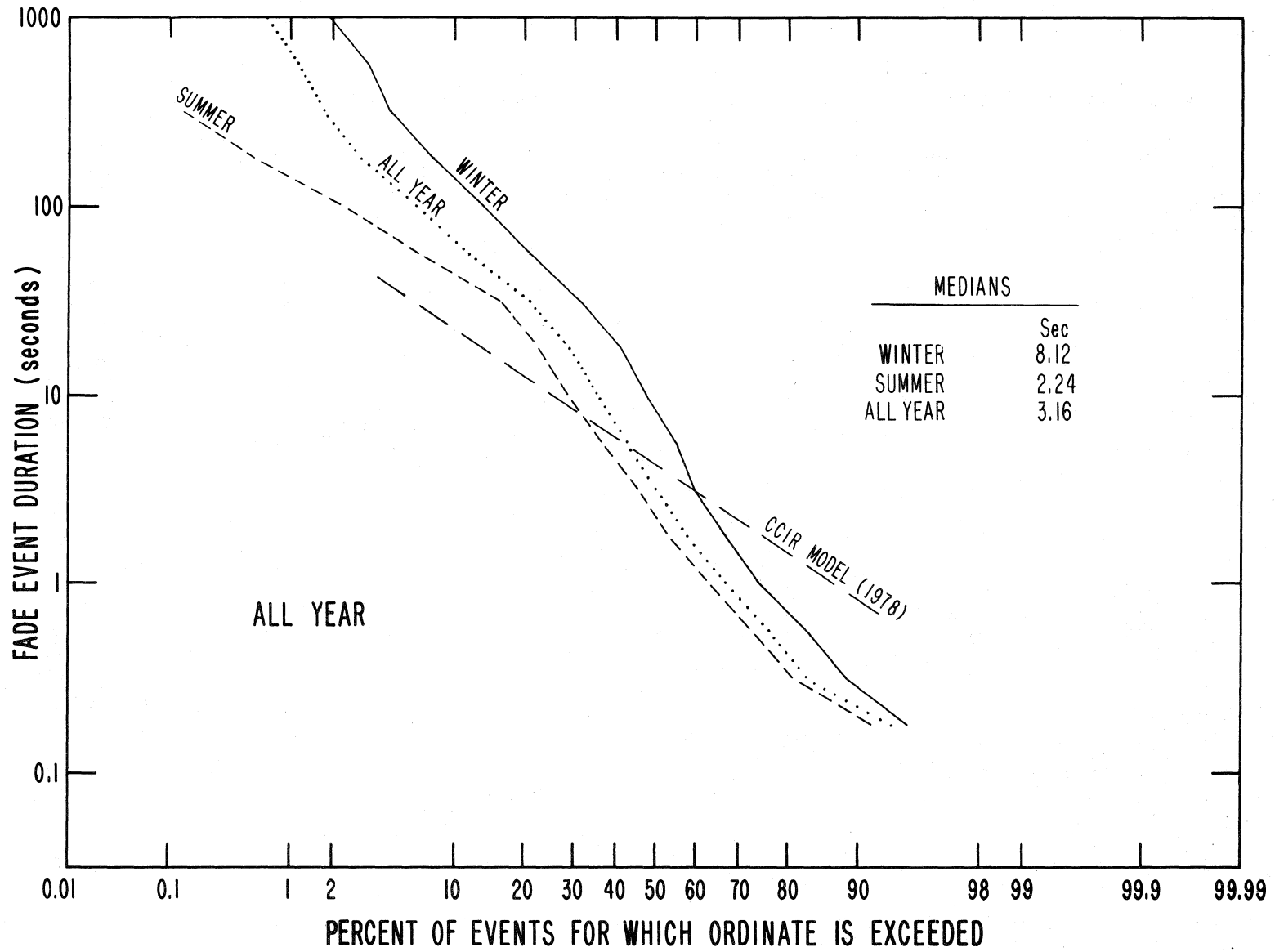Figure 9.   Fade event duration distributions for summer time blocks.

Figure 10. Fade event duration distributions for all hours.

Table 3. Fade Event Duration Statistics for Paths A and B,
Swingate - Houtem

Fade Event Durations

	Hours	Median seconds	Mean seconds	St. Dev.**	Total Number of Fade Events
Winter:	00 - 06	6.8	3.8	9.1	91
	06 - 13	12.0	6.7	11.7	123
	13 - 18	6.9	6.1	10.1	91
	18 - 24	9.0	5.0	9.7	109
Summer:	00 - 06	3.2	2.3	7.3	148
	06 - 13	1.5	1.6	8.4	162
	13 - 18	2.0	2.0	9.4	235
	18 - 24	2.6	2.5	9.3	236
Winter:	all hours	8.1	5.4	10.3	414
Summer:	all hours	3.5	2.1	8.8	781
All Year:	all hours	3.2	2.9	9.5	1195

In terms of diurnal variations, the winter data show the
longest median fade event durations for morning hours (0600 -
1300), while in summer the longest median fade event durations
occur during night and early morning hours (0000 - 0600). This
may be related to atmospheric effects during and after sunrise
which generally occurs after 0600 in winter and before 0600 in
summer at the latitude where the path is located. Data are not
available for diurnal variations in the refractivity gradients
that could be associated with the fade event statistics.

The summary cumulative distributions of fade event duration
in Figure 10 are compared with a theoretical curve based on a
(long-term) median individual fade duration of 4.26 s derived
from (11) in CCIR Report 338-3 (1978). The same report cites a
standard deviation of $10 \log_{10} (3.6 s) = 5.6$ in accordance with
Bullington's work (1971). Note that the all-year median fade
event duration from Table 3 is less than the CCIR estimate for
the median duration of individual fades.

**Standard deviations are expressed in terms of 10 times the
logarithm (to the base 10) of the duration ratio.

19

We have already noted that individual fades for the Swingate - Houtem path are frequently shorter in duration than fade events. Although it is not possible to recover the statistics of individual fades from the cassette records, the comparison of fade event durations with signal level distributions for the -75 dBm threshold level permits an estimation of the relation between the number and the duration of individual fades and fade events. A sample analysis was conducted for typical summer and winter data; also, some of the fade event strip charts are available for inspection. The example shown in Figure 7 is somewhat extreme since there are 8 individual fades, each lasting about 1 s or less, for the single 47.3 s fade event on receiver A.

This sample analysis resulted in median values of 2.3 individual fades per fade event for the summer example, and 2.1 for the winter example. Consequently, on the average there will be at least twice as many individual fades as fade events. Also, the median duration of individual fades is likely to be not more than about one-half of the median of the fade events. Even in the absence of information permitting more complete statistical analyses, it would appear that the CCIR model tends to overestimate median fade duration for this path, and possibly for other paths of this type; i.e., long over-water links in the 4 to 5 GHz frequency range. A comparison of the slopes for the theoretical and the measured distributions shown in Figure 10 is not appropriate because of the bias introduced by the measurement methods.

5. APPLICABILITY OF RESULTS TO SYSTEMS IN OTHER AREAS

The microwave communication link evaluated in this report is somewhat atypical because of its length (88 km) and environment (across water). It is, however, possible to apply the results to other over-water and coastal areas since fading characterisitcs are related to terrain and atmospheric stratification. A measure of the latter are statistics of refractivity gradients. Detailed gradient statistics for the exact path location during the measurement period could not be obtained.

20

The points closest to the path for which long-term cumulative distributions of the refractivity gradients are available are Cardington, England (north of London), and Brussels, Belgium (Samson, 1975). At these two locations, ground-based super-refractive layers (N-units/km < -40) at least 100 m thick occur for 60 to 70% of the observations (twice daily at Brussels and four times daily at Cardington). Also, gradients more negative than -250 N-units/km were observed for approximately 0.1% of the occurrences at Cardington in the groundbased layer up to 500 m above ground.

The compilations of gradient statistics prepared by Samson (1975, 1976) illustrate the preponderance of super-refractive gradients in most coastal locations in the United States. Examples of locations for which such gradients in the ground-based 100-m layer occur during at least 25% of the observations are Anchorage and Barrow, Alaska; Long Beach, Oakland, and San Diego, California; Key West and Miami, Florida; Washington, D.C.; Hilo, Hawaii; Caribou, Maine; New York, N.Y.; Cape Hatteras, North Carolina; Seattle, Washington; and Browns-ville, Texas. Even ducting gradients are relatively frequent at these locations with the highest incidence found at Hilo and Cape Hatteras (>9%).

It may therefore be concluded that the results of the measurement program described here may be applicable to most coastal areas in North America and to links in Pacific Island chains. We must remember, however, that the path discussed here is unusually long for a line-of-sight link, and that the antennas for the line-of-sight situation are by necessity high above the surface.

The results could also be applied to some inland locations in continental climates where the path extends over relatively smooth terrain and super-refractive gradients exist for appreci-able fractions of the observations. Examples, during the summer months, are Denver, Colorado; Bismarck, North Dakota;

21

and Dayton, Ohio. However, terrain influences the homogeneity of the gradient structure, and a careful study of the terrain is essential in these cases.

6. CONCLUSIONS

The purpose of this study is to check the measurement results against available prediction models, particularly those recommended by the CCIR. Agreement between predicted signal level distributions and those derived from the measurements is fair in the deep fading region where the CCIR model applies. The results, if representative of a full year, do not confirm the validity of extrapolating from worst month to all year on the basis of annual mean temperature as suggested by Vigants (1975). However, the maritime climate characteristics of the path environment tend to lessen seasonal changes and make the concept of a "worst month" less applicable.

Because of the limitations in the measurement techniques, precise statistics of individual fades could not be obtained. From the analyses and reasoning described in Section 4, it appears that the median duration of individual fades is not more than approximately <u>one-half</u> of that expected from available fade event models. Total fade event durations are longer in winter than in summer while the number of fade events is larger in summer.

Assuming that fading characteristics are primarily a function of refractivity gradient statistics, the results of the measurement program are applicable almost universally over water or smooth coastal terrain since the gradient distributions for the area of the path are not unique. Because of its length, however, the path is not typical of overland communication links. Since the super-refractive gradients that favor fade events occur frequently even inland in continental climates, allowance for substantial fading must be made for long links unless the terrain can be expected to inhibit homogeneous stratification over the path area.

Finally, the measurement results confirm the usefulness of the original design concept for this path. Because of the link

length and inadequate clearance (under generally accepted standards), extensive fading exists on the nominally line-of-sight paths between the upper antennas. The quadruple diversity system utilizing paths between lower antennas that are normally blocked, but can become active during ducting conditions, appears to work well, and insures adequate communication reliability. It is reasonable to expect that similar designs will work equally well in most coastal or maritime environments where super-refractive gradients exist for large fractions of the time.

7. ACKNOWLEDGEMENTS

8. REFERENCES

Barnett, W.T. (1972), Multipath propagation at 4, 6, and 11 GHz, Bell System Tech. J., 51, No. 2, 321 - 361.

Bullington, K. (1971), Phase and amplitude variations in multipath fading of microwave signals, Bell System Tech. J., 50, No. 6, 2039 - 2053.

CCIR (1978), Propagation data required for line-of-sight radio-relay systems, Report 338-3, Documents of the XIV Plenary Assembly (ITU, Geneva).

Morita, K. (1970), Prediction of Rayleigh fading occurrence probability of line-of-sight microwave links, Rev. Elect. Comm. Lab., NTT, Japan, 18, 11 - 12.

Norton, K.A., P.L. Rice, and L.E. Vogler (1955), The use of angular distance in estimating transmission loss and fading range for propagation through a turbulent atmosphere over irregular terrain, Proc. IRE 43, No. 10, 1488 - 1526.

Samson, C.A. (1975), Refractivity gradients in the northern hemisphere, OT Report 75-59, Office of Telecommunications (Supt. of Documents, U.S. Government Printing Office, Washington, D.C. 20402).

Samson, C.A. (1976), Refractivity and rainfall data for
    radio systems engineering, OT Report 76-105, Office of
    Telecommunications (Supt. of Documents, U.S. Govern-
    ment Printing Office, Washington, D.C. 20402).

Vigants, A. (1975), Space diversity engineering, Bell System
    Tech. J., 54, No. 1, 103 - 142.

White, R.F. (1970), Engineering considerations for microwave
    communications systems, Lenkurt Electric Co., Inc.,
    San Carlos, California.

Zebrovitz, S. (1975), The use of multiple diversity to
    minimize the effects of ducting on a long microwave
    path, Nat. Telecomm. Conf. 1975, Conference Record,
    10-23 - 10-28, (IEEE, New York, N.Y.).

BIBLIOGRAPHIC DATA SHEET

	1. PUBLICATION OR REPORT NO. NTIA Report 79-30	2. Gov't Accession No.	3. Recipient's Accession No.
4. TITLE AND SUBTITLE SIGNAL LEVEL DISTRIBUTIONS AND FADE EVENT ANALYSES OF A 5 GHz MICROWAVE LINK ACROSS THE ENGLISH CHANNEL			5. Publication Date October 1979
			6. Performing Organization Code NTIA/ITS
7. AUTHOR(S) D. R. Wortendyke, A.P. Barsis and R.R. Larsen			9. Project/Task/Work Unit No. 9108240/9103484
8. PERFORMING ORGANIZATION NAME AND ADDRESS U.S. Department of Commerce, National Telecommunications and Information Administration, Institute for Telecommunication Sciences, Boulder, CO 80303			10. Contract/Grant No.
11. Sponsoring Organization Name and Address ITS 1842nd E.E.G. U.S. Dept. of Commerce USAF Boulder, CO 80303 Scott AFB, IL			12. Type of Report and Period Covered NTIA – T.R.
			13.

14. SUPPLEMENTARY NOTES

15. ABSTRACT (A 200-word or less factual summary of most significant information. If document includes a significant bibliography ot literature survey, mention it here.)

This report describes instrumentation for fading studies and measurement results over an 88-km multiple-diversity line-of-sight microwave link across the English Channel operating in the 4 to 5 GHz frequency range. Signal level and fade duration statistics derived from the measurements are compared with CCIR models. It is found that median fade duration tends to be less than estimates from the CCIR models.

16. Key Words (Alphabetical order, separated by semicolons)

Automatic signal monitoring; 5 GHz signal levels; microwave fading; multiple diversity receivers.

17. AVAILABILITY STATEMENT [x] UNLIMITED. [ ] FOR OFFICIAL DISTRIBUTION.	18. Security Class (This report) Unclassified	20. Number of pages 27
	19. Security Class (This page) Unclassified	21. Price.